

Electrical Conduction and Diffusion Studies in $\text{NH}_4\text{H}_2\text{PO}_4$ and KH_2PO_4 Single Crystals

M. SHARON AND ANJAN K. KALIA

Department of Chemistry, University of Poona, PUNE 411 007, India

Received September 27, 1976; in revised form January 25, 1977

Electrical conduction (dc) studies are made with pure and cobalt(II)-doped single crystals of $\text{NH}_4\text{H}_2\text{PO}_4$ and KH_2PO_4 . The effect of the dopant concentration on the enthalpy for the migration of protons and the enthalpy for the rotation of the H_2PO_4 group have been studied. It is suggested that proton migration occurs through a synchronous phosphate rotation mechanism. Tritium diffusion studies in KDP and $^{32}\text{PO}_4$ diffusion in ADP crystals have been made. The mechanisms for the conduction and diffusion processes are found to be different in nature. The distribution coefficients of Co(II) dopant in ADP (2.92×10^{-3}) and KDP (1.14×10^{-3}) are calculated. The following enthalpy values are obtained.

	KDP (eV)	ADP (eV)
Enthalpy for the migration of protons	0.01 ± 0.01	0.15 ± 0.02
Enthalpy for the rotation of phosphate group	0.71 ± 0.01	0.66 ± 0.01
Enthalpy for T-diffusion	0.14 ± 0.01	—
Enthalpy for $^{32}\text{PO}_4$ diffusion	—	0.24 ± 0.01

Introduction

There are many papers on ammonium dihydrogen phosphate (ADP) and potassium dihydrogen phosphate (KDP) crystals to suggest that these crystals are protonic conductors (1-12). Efforts have also been made by these authors to explain a plausible mechanism for the proton conduction in such hydrogen-bonded crystals. Murphy (7) considered the possibility of L and D defects to explain the conduction in ADP, while Harris and Vella (8-9), in analogy with the Herrington-Staveley (13) model for NH_4Cl , introduced A-defects along with L-defects. The presence of these point defects (i.e., L and A), however, requires the existence of extrinsic and intrinsic regions in the conductivity plots. But the experimental observations of conductivity data are in dispute: Some authors report the presence of intrinsic and extrinsic regions (3-5, 7), whereas some report the absence of these regions (8).

Because of these ambiguities, the enthalpies for the conduction processes are in dispute as well. It is, therefore, necessary to look at these crystals from a completely different angle. First, the dc conductance of pure as well as doped (of varied concentration) ADP and KDP crystals should be studied over a wider temperature range (+180 to -180°C). The low-temperature measurement is expected to show the extrinsic region (if there is one).

If these crystals are doped with a divalent impurity, each dopant is expected to create at least one vacancy, thus making possible the formation of (impurity-vacancy) complexes, which are expected to affect the conductivity data. Therefore, if the conduction process is controlled by the classical defect concept (as has been envisaged (7-9, 13)), one may expect to observe an enthalpy for the association of such complexes as well as a positive value for the association constant of such complexes (17). Furthermore, the doped crystal should show an extrinsic region and one should be

able to calculate the enthalpy for the migration of the defect, which should be much smaller than the enthalpy for the formation of defects. These can be examined by applying Lidiard's isotherm (17) equation to the conductance data of ADP and KDP single crystals.

Nevertheless, if these calculations are found to be inapplicable to KDP and ADP crystals, a different approach to the mechanism of the conduction process should be made. Blinc *et al.* (20, 21) have made NMR studies on KDP single crystals and have found two types of frequencies, one due to phosphate rotation (temperature dependent) and the other to proton jump frequency (temperature independent).

It is, therefore, desirable to study the dc conduction with pure and doped single crystals of ADP and KDP containing varied amounts of dopant concentrations. In order to have a full comprehensive study, tritium diffusion in KDP (in the temperature range 40–160°C) and phosphate diffusion in ADP are also desirable. These studies could throw light on the disputed mechanism for the conduction and diffusion processes in ADP and KDP crystals. The present paper deals with these studies.

Experimental Technique

A. Growth of ADP and KDP Single Crystals

The single crystals of pure ADP and KDP were grown by the slow-evaporation technique at pH 3.8–4.2 and 4.2–4.4, respectively. Crystals doped with cations (cobalt(II)) were grown at pH 3. In order to measure the concentration of dopant in each crystal, Co-60 tracer was used. The specific activities of the crystals and the mother liquor were measured. By comparing the activity of the added tracer with the amount of added inactive cobalt phosphate, the number of cobalt atoms present in the mother liquor per gram and the number of cobalt atoms present in each crystal were calculated. The measurement of the activities was made by a low anticoincidence GM counter (ECIL, India). The distribution coefficients of cobalt in the crystal were found to be 1.14×10^{-3} and 2.92×10^{-3} for KDP and ADP, respectively. Weis (16) also found a distribution coefficient of 7.7×10^{-3} for the ADP

crystal, which is of the same order as that observed here.

B. dc Conductance Measurements

The cell used to measure the dc conductance of the single crystal is shown in Fig. 1. The cell was made of two units. The lower unit consisted of a stainless steel electrode P_2 inserted into a Teflon disk G (1.2-cm diameter) which in turn was embedded into a stainless steel guard disk W (2.0-cm diameter). The central electrode P_2 has a flat disk (0.6-cm diameter) in the front and a nut bolt arrangement in the back. A fine stainless steel spring K, placed in the cavity of the Teflon disk G, provided a constant pressure on electrode P_2 . The upper unit of the cell was identical to the lower unit except that disks G and W were replaced by a single Teflon disk T, which had an additional hole X for inserting the thermocouple. The crystal L ($1.3 \times 1.3 \times 0.2$ cm³) was sandwiched between the two units using four nut-bolt spring arrangements S.

To obtain perfect contact between the crystal and the electrodes (P_1, P_2) a thin film M of aluminium was deposited on each side of crystal L by vacuum deposition technique. The area of the aluminium-deposited surface was exactly equal to the area (0.27 cm²) of the electrodes P_1 and P_2 . The outer area of the crystal resting on the guard disk W had no aluminium deposition. After crystal was fixed in the electrode unit, it was inserted into a glass assembly (Fig. 1B) made from B-30 cones per socket. The inner wires of H and D were connected to the P_1 and P_2 electrodes and the outer screening E of wire D was connected to guard disk W. The chromel–alumel thermocouple (X^1) was inserted in the cavity X of the cell (Fig. 1A). The clamp-spring arrangement S_2 was used to tighten the B-30 cone with its B-30 socket.

The electrical connections are shown in Fig. 1C. The guard disk W acted as a guard ring against the surface conduction. The electrode P_1 was connected to the collective electrode H of the vibrating condenser electrometer F (ECIL EA 812, India). The electrode P_2 was connected to the positive terminal of the stabilized power supply Z (Aplab, India) through wire D. The negative terminal of the

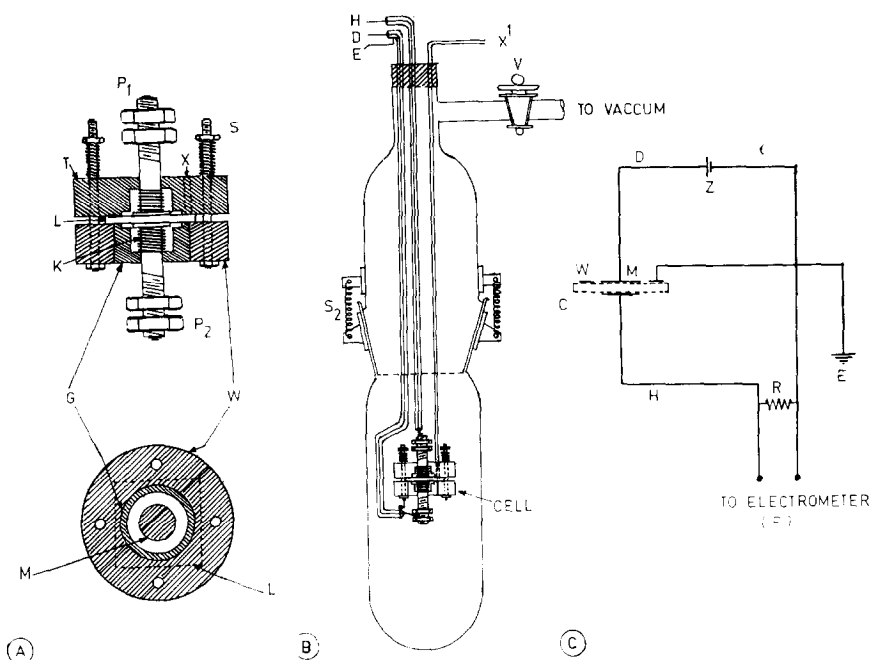


FIG. 1. Schematic diagram of a dc conductivity cell.

power supply Z, along with the shielding wires of all the cables, was grounded. The negative terminal of the 2.0-V power supply connected to the potentiometer was also grounded. This was essential, to eliminate the induction effects on the electrometer readings. The low-temperature measurements were made under a constant vacuum, whereas the high-temperature measurements were made in nitrogen atmosphere. But neither nitrogen gas nor the vacuum condition produced a change in the conductance. The conductance of the crystal at any temperature in the range -72 to 170°C was measured after the crystal had attained a constant temperature for about 10–15 min. A potential of 10 V was then applied across the crystal for 3–5 min and the corresponding value of the current passing through the electrometer was noted, from which the specific conductance (σ) of the crystal was calculated. The dc conduction measurements were made along the (100) plane. The plot of $\log(\sigma T)$ versus $1/T$ is shown in Fig. 2 for KDP crystals containing 73, 198 and 435 ppm of Co(II), respectively, and in Fig. 3 for ADP crystals containing 144, 216, 690, and 740 ppm of Co(II). The method of least squares was used for calcu-

lating the standard deviation, slopes, and intercepts of linear plots.

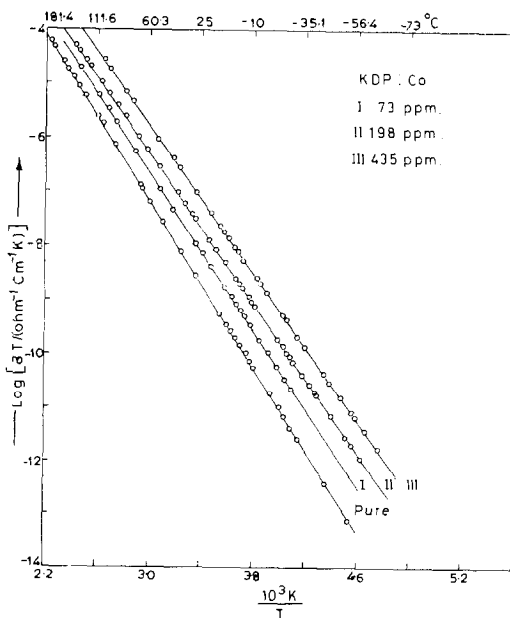


FIG. 2. Variation of $\log(\sigma T)$ with $1/T$ for pure and Co^{2+} -doped KDP single crystals.

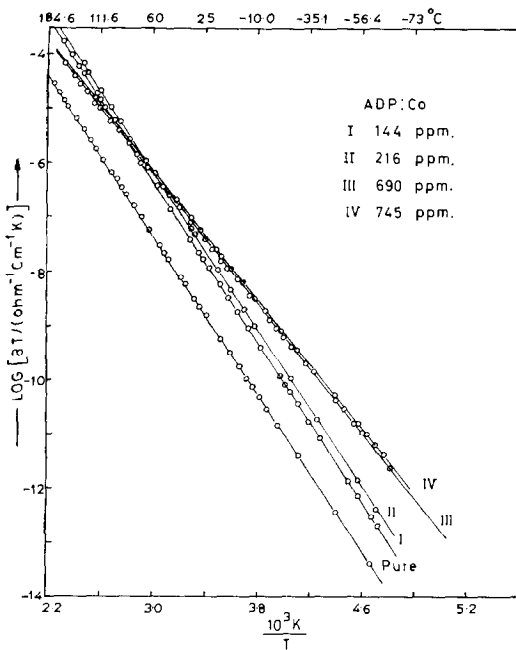


FIG. 3. Variation of $\log(\sigma T)$ with $1/T$ for pure and Co^{2+} -doped ADP single crystals.

C. Experimental Technique for Tracer Diffusion

The sectioning technique was used for studying the tracer diffusion in ADP and KDP crystals using a microtome. The brass anvil A

was prepared on which the optically flat mirror M_1 was fixed by means of a metallic strip screw arrangement R. The crystal C was attached to anvil A, by means of specially prepared Teflon holder T, which had a cavity machined to match the shape and size of crystal C, such that when Teflon block T was placed over crystal C about 2–3 mm of the top layer of the crystal was projected out. Crystal C was rubbed to achieve the particular shape of Teflon block T. Two screws S_1 and S_2 were used to fix block T to anvil A. Anvil A was fixed in microtome chuck B. The reproducibility of the crystal position with respect to the knife was achieved by a lamp and scale arrangement (Fig. 4). This arrangement could measure the change in the crystal position by $\pm 1.0 \mu\text{m}$.

A labeled salt solution of $1.0 \mu\text{l}$ was slowly (in steps) applied to the crystal surface. After it was annealed in nitrogen, the crystal was slowly cooled to room temperature and sectioned, and $5.0\text{-}\mu\text{m}$ cuttings were collected. For studying the diffusion of $^{32}\text{PO}_4^{3-}$, an aluminum planchette containing the sectioned material was counted by an anticoincidence GM counter (GCS16 ECIL, India). For the tritium activity measurements, to each vial containing $5.0\text{-}\mu\text{m}$ cuttings of the crystal, 15.0 ml of dioxane, 2.0 ml of liquid scintillator NE 210, and 2.0 g of silica gel (TLC grade) were

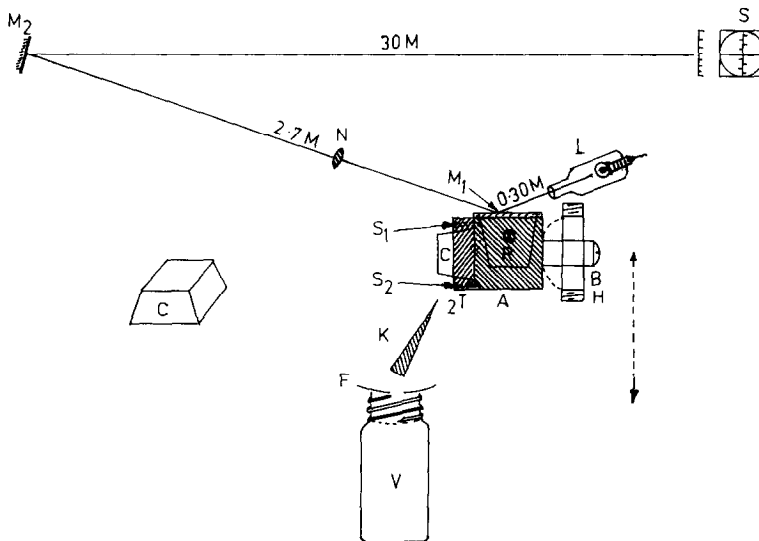


FIG. 4. Experimental arrangement for a sectioning crystal.

added. All the vials were shaken thoroughly to disperse the sectioned material homogeneously with silica gel and then counted by a liquid scintillation coincidence counter (ECIL). The efficiency of tritium counting was found to be 32%. The log (activity, counts per minute) was then plotted versus the square of thickness to calculate the diffusion coefficient using Eq. (1):

$$C = \frac{C_0}{(\pi Dt)^{1/2}} \exp(-x^2/4 Dt), \quad (1)$$

where C and C_0 are the activities of the tracer at thicknesses x and $x = 0$, respectively. D and t are the diffusion coefficient and the time of annealing, respectively. These studies were made at different temperatures and diffusion coefficients for each temperature were calculated. Finally, the log (diffusion coefficient) was plotted against $1/T$. From the slope and intercepts of the linear plot, the enthalpy and entropy for the diffusion process were calculated by using the equation

$$D = D_0 \exp(-E_d/kT), \quad (2)$$

where

$$D_0 = \frac{z a^2}{z_1} v_0 \exp(\Delta S/k) \quad (3)$$

and a , v_0 , ΔS , and E_d are the lattice distance, Debye frequency, entropy, and enthalpy for diffusion, respectively. Depending upon the crystal structure, z_1 and z are constants.

D. Comparison of Tracer Diffusion Coefficient with Ionic Conductivity

Considering the ionic conductivity and self-diffusion in crystal to be controlled by the same mechanism, Einstein derived relationship (5) from Eq. (4); i.e.,

$$\frac{\sigma}{D} = \frac{N e^2 v_\sigma a^2 \exp(-E_\sigma/kT)}{kT v_D a^2 \exp(-E_D/kT)}, \quad (4)$$

where

N = Avogadro number,

e = charge of carrier,

v_σ and v_D = frequencies for conductance and diffusion, respectively,

E_σ and E_D = Activation energies for conduction and diffusion processes, respectively,

σ and D = Specific conductance and diffusion coefficient at temperature T ,
 k = Boltzman constant.

If v_σ , v_D , E_σ , and E_D are the same then Eq. (4) reduces to

$$\sigma/D = Ne^2/kT. \quad (5)$$

Now using Eq. (5), theoretically expected values of the diffusion coefficient (D_{expected}) can be calculated from the conductivity data (experimentally observed) and vice versa. Therefore, if the conductivity and the diffusion processes in KDP and ADP crystals are controlled by the same mechanism, then a plot of $\log(D_{\text{expected}})$ vs $1/T$ should be parallel to the plot of $\log(D_{\text{experimental}})$ vs $1/T$. This comparison is shown in Fig. 5. for $^{32}\text{PO}_4^{3-}$ diffusion in the ADP crystal and for the tritium diffusion studies in KDP (Fig. 6). The non-parallel behavior of the plots is obviously due to different values of E_σ and E_D (Table I). However, when the exponential terms (Eq. (4)) were included in the Einstein relation (assuming $v_D = v_\sigma$) the D_{expected} plot became parallel to the experimentally observed values (Fig. 6). In principle, however, the two graphs should have been superimposed on each other

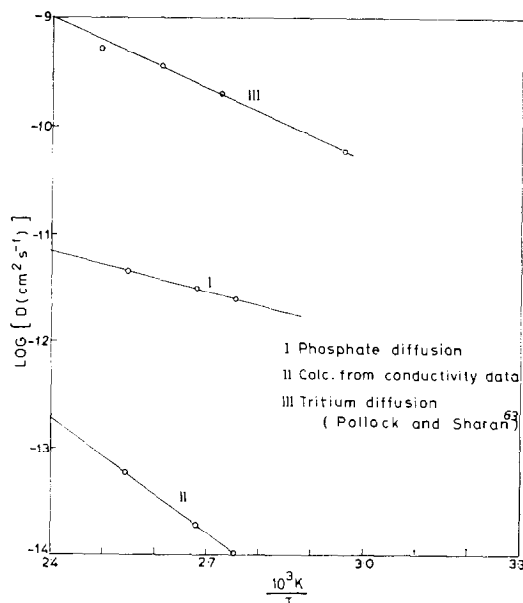


FIG. 5. Comparison of $\log D$ against $1/T$ plots for an ADP single crystal.

TABLE I

Substance	E_{obs} (eV)	A ohm ⁻¹ cm ⁻¹	ΔS (eV °K ⁻¹)	H_s (eV) ^a	H_a (eV)	H_m (eV)	E_{DT}	D_0 cm ² Sec ⁻¹	ΔS_D eV Kg ⁻¹
KDP pure	0.76 ± 0.02	2.487 × 10 ⁴	-1.33 × 10 ⁻⁴	+0.10 ± 0.01	-0.03 ± 0.02	0.71 ± 0.01	0.14 ± 0.02	238 ± 10 ⁻⁹	-1.28 × 10 ⁻³
+73 ppm Co ²⁺	0.72 ± 0.02	2.19 × 10 ⁴	-1.43 × 10 ⁻⁴						
+198 ppm Co ²⁺	0.69 ± 0.02	1.29 × 10 ⁴	-1.86 × 10 ⁻⁴						
+435 ppm Co ²⁺	0.68 ± 0.03	2.48 × 10 ⁴	-1.22 × 10 ⁻⁴						
ADP pure	0.73 ± 0.04	5.52 × 10 ³	-2.56 × 10 ⁻³	+0.15 ± 0.02	-2.11 ± 0.07	0.66 ± 0.01	0.24 ± 0.01	8.24 × 10 ⁻⁹	-1.07 × 10 ⁻³
+144 ppm Co ²⁺	0.73 ± 0.05	5.92 × 10 ⁴	-6.20 × 10 ⁻³						
+216 ppm Co ²⁺	0.70 ± 0.04	5.92 × 10 ⁴	-6.20 × 10 ⁻³						
+690 ppm Co ²⁺	0.59 ± 0.03	5.52 × 10 ²	-4.44 × 10 ⁻³						
+745 ppm Co ²⁺	0.59 ± 0.03	5.88 × 10 ²	-4.38 × 10 ⁻³						

^a H_s ≈ enthalpy for migration of protons. H_m ≈ enthalpy for rotation of H₂PO₄⁻ group. H_a ≈ enthalpy for association of (impurity-vacancy) complex.

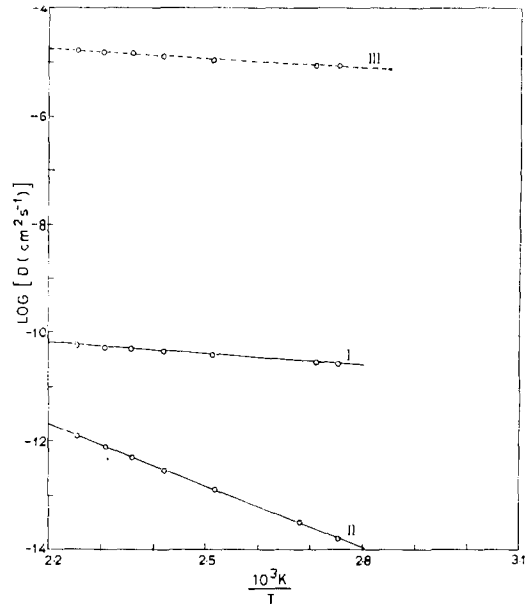


FIG. 6. Log D against $1/T$ plots for a KDP single crystal (I) observed from tritium diffusion; (II) calculated (from σT using Nernst-Einstein relation); (III) calculated (from σT by including exponential function in Nernst-Einstein relation).

but they are separated by a large factor. This may be due to the fact that the assumption $v_D = v_\sigma$ may also not be valid for these crystals.

Results

1. Potassium Dihydrogen Phosphate

Figure 2 shows no break in the conductivity plot for either pure or doped crystals. The conductivity of pure crystal at 25°C was found to be 5.97×10^{-12} ohm⁻¹ cm⁻¹ and varies exponentially with temperature according to the equation

$$\sigma T = 2.487 \times 10^4 \exp\left(\frac{-0.76 \pm 0.02}{kT}\right) \text{ ohm}^{-1} \text{ cm}^{-1} \text{ k.} \quad (6)$$

The enthalpy for conduction E_{obs} , the preexponential function A , and the entropy change are given in Table I. In order to calculate the enthalpy for the migration of proton and the enthalpy for the association of the vacancy-impurity complex, isotherm calculations (as discussed by Lidiard (17)) were made. The

conductivity isotherms were plotted for (σ_c/σ_0) versus dopant concentration c by using equation (Fig. 7)

$$c = (\theta + 1) \frac{\sigma_c}{\sigma_0} x_0 + x_0^2 K_2(T) (\theta + 1)^2 \left(\frac{\sigma_c}{\sigma_0} \right)^2, \quad (7)$$

where σ_0 and σ_c are the specific conductance for pure and doped crystals with concentration c , respectively. x_0 and $K_2(T)$ are the number of intrinsic defects at temperature T and the association constant for the (impurity–vacancy) complex formation. The ratio of the mobility of two complementary types of defects present in the crystal is represented by θ . These isotherms meet at $c = 0$, suggesting that $\theta = 0$. Like NaCl, in KDP and ADP, the conduction is due to protons (cation) only, and hence one of the two complementary defects in ADP/KDP is absent. Therefore, one expects the conduction to be zero or unity. Therefore, $c/(\sigma_c/\sigma_0)$ was plotted versus (σ_c/σ_0) for different temperatures and gave a linear plot. From the slopes ($x_0^2 K_2(T)$) and the intercepts (x_0), of these linear plots the values of x_0 and $K_2(T)$ were calculated for different temperatures. The enthalpy H_s for the formation of

intrinsic defects was then calculated from the slope of the linear plot of $\log(x_0)$ vs $1/T$ using the equation

$$x_0^2 = \exp(-H_s/kT) \quad (8)$$

which is 0.1 ± 0.01 eV. Similarly the enthalpy for the association of the (impurity–vacancy) complex was calculated from the slope of the linear plot of $\log(K_2)$ vs $1/T$ using the equation

$$K_2(T) = z^1 \exp(H_s/kT) \quad (9)$$

which gives a negative value of 0.033 ± 0.02 eV. Assuming the applicability of the equation $E_{\text{obs}} = 0.5 H_s + H_m$ (in the absence of any knee, such an assumption may not be valid) and substituting the values of E_{obs} and H_s , H_m is 0.71 ± 0.01 eV. These calculations are made on the assumption that the classical defect mechanism operates in these crystals. The validity of these calculations is discussed in detail below.

Tritium diffusion studies. The equation for tritium diffusion was found to be

$$D = 2.38 \times 10^{-9} \exp\left(-\frac{0.14 \pm 0.02 \text{ eV}}{kT}\right) \text{ cm}^2 \text{ sec}^{-1}.$$

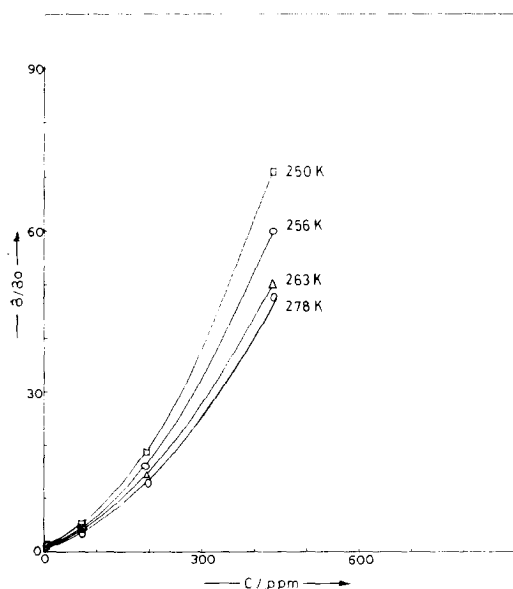


FIG. 7. Conductivity isotherms for a Co^{2+} -doped KDP single crystal.

The value of the enthalpy for the diffusion E_{DT} process ($0.14 + 0.02$ eV) is comparable to the value of 0.16 eV reported by Hoffmann and Lieser (15), who studied tritium diffusion in the temperature range -27 to $+40^\circ\text{C}$. The entropy value for the diffusion process calculated from D_0 is $-1.28 \times 10^3 \text{ eV}^\circ\text{K}^{-1}$. Failure in obtaining a parallel line for the plot of $\log(D)$ versus $1/T$ (calculated from Einstein relationship) with $\log D$ versus $1/T$ (experimentally observed) and getting a parallel line between $\log D_{\text{cal}}$ and the $1/T$ plot (after including the exponential enthalpy terms for the conduction and diffusion processes in the Einstein relationship) with $\log(D_{\text{observed}})$ vs $1/T$ suggests that the mechanisms for the conduction and the diffusion processes, are completely different from each other.

2. Ammonium Dihydrogen Phosphate

The conductivity of a pure crystal at 298°K was found to be $5.32 \times 10^{-12} \text{ ohm}^{-1} \text{ cm}^{-1}$

which is about 40-fold lower than the value observed by Perrino and Wentreck (11). The value of conductivity at any temperature (-70 to $+165^\circ\text{C}$) is given by the relation

$$\sigma T = 5.52 \times 10^3 \exp\left(\frac{-0.73 \pm 0.02 \text{ eV}}{kT}\right) \text{ ohm}^{-1} \text{ cm}^{-1} \text{ k.}$$

The enthalpy of conduction E_{obs} , preexponential function A , and entropy change are given in Table I. The isothermal calculations were carried out in a similar manner as was performed for KDP and the conductivity isotherm plot for (σ_c/σ_0) vs c at different temperatures are shown in Fig. 8. But these isotherms do not meet at $c = 0$ (as observed with KDP), which is an indication (17) for the presence of some unaccounted impurity (c_0) in the crystal. The value c_0 was calculated from the point where the isotherms of σ_c vs c meet at the x axis and is 60 ppm. Therefore for all subsequent calculations $c + c_0$ was taken as the true impurity concentration. As with KDP a negative value for $K_2(T)$ was obtained, with an association enthalpy H_a of -2.11 ± 0.07 eV. The enthalpy

H_s for the formation of intrinsic defects is $+0.15 \pm 0.02$ eV, which is of the same order as that observed for KDP (0.1 ± 0.01 eV). The enthalpy for the migration of protons is 0.66 eV as compared to 0.71 eV obtained for KDP.

Diffusion studies. Phosphate diffusion studies in the temperature range 90 to 120°C were made. The enthalpy for phosphate diffusion is found to be 0.24 ± 0.01 eV, which is higher than the value of 0.14 ± 0.01 eV observed for the tritium diffusion in KDP. The entropy value (-1.07×10^{-3} eV $^\circ\text{K}^{-1}$) is a negative quantity. The general diffusion equation for phosphate is

$$D = 8.24 \times 10^{-9} \exp\left(\frac{-0.23 \pm 0.01 \text{ eV}}{kT}\right) \text{ cm}^2 \text{ sec}^{-1}.$$

Since this crystal is a pure protonic conductor it is expected that the enthalpy for phosphate diffusion should be higher than enthalpy for tritium diffusion (8) (0.4 eV) and should also be higher than enthalpy for the conduction process. More investigation is, therefore, required before one can comment on this result.

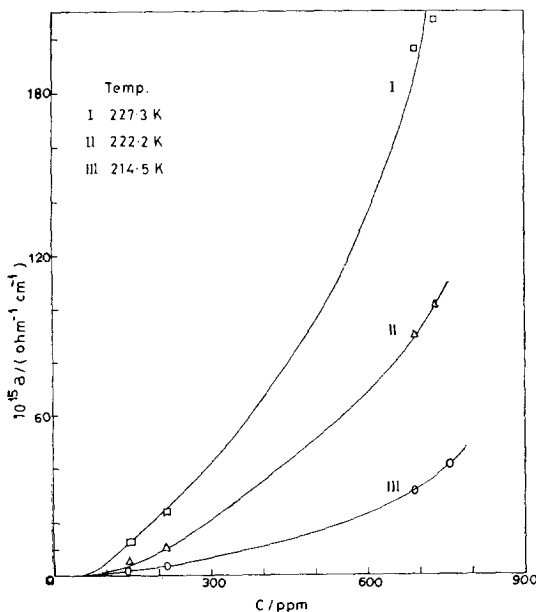


FIG. 8. Conductivity isotherms (σ_c/σ_0 vs C) for a Co^{2+} -doped ADP single crystal.

Discussion

1. KDP

It is rather difficult to compare the present values of enthalpies for conduction with that of O'Keeffe and Perrino (4) who observed a knee at 180°C (which is due to phase transition (18)) and that of Harris and Vella (9) who observed a knee at 100°C (which is due to some decomposition (19)). Nevertheless O'Keeffe and Perrino did not observe any knee below 180°C , but the enthalpy (E_{obs}) for temperature below 180° is lower (0.55 eV) than the value (0.76 eV) observed in the present work.

The presence of water vapor and the absence of any guard ring might have resulted in surface conduction to show a low-activation energy while in the present work the modified guard ring and dry nitrogen atmosphere would have eliminated these effects. The measurements by Harris and Vella (9), could cause dc electrolysis of the crystal because they applied potential for more than 30 min in taking each

reading, whereas in the present work it was applied only for 5 min.

The value of conductivity was found to increase with the increase of dopant concentration but the enthalpy for conduction followed the reverse trend. O'Keeffe and Perrino (4-5, 8) observed a similar trend with the HSO_4^- dopant except that the enthalpy for conduction remained independent of the anion dopant concentration. Since the enthalpy for the conduction depends upon the dopant concentration (a property of intrinsic region) and the enthalpy for migration of protons is very high (Table I), it is reasonable to assume that the conductivity plots of the temperature region from -70 to $+160^\circ\text{C}$ is neither an extrinsic nor an intrinsic region.

2. ADP

Like KDP, ADP also showed the absence of any break in the conductivity plot. This is in accordance with the results of Harris and Vella, (9) and Pollock and Sharan (8); Murphy (2), and Perrino and Wentreck (10) on the other hand, observed the presence of a knee around $84-87^\circ\text{C}$. Murphy has further reported that with substantially pure crystals the overheating resulted in the elimination of a knee with an increase of the conductivity value and that Ba^{2+} - and SO_4^{2-} -doped crystals do not show the presence of any knee. The absence of a knee and the reproducibility of the results between -70 and $+160^\circ\text{C}$ in the present work confirm that the evolution of ammonia (as suggested by Harris and Vella (9)) does not affect the conductivity data. Therefore it can be concluded that the hydrogen of ammonia does not contribute toward the conduction in ADP. The enthalpy for conduction E_{obs} $0.75 + 0.04$ eV is higher than the values 0.68, 0.63, and 0.54 eV reported by Harris (9), Murphy (7), and Perrino (10), respectively. This suggests that our crystal must be purer than theirs. Our low conductivity values (compared to Perrino (10)) may also be due to the high purity of the crystal, because the values of conductivity increase with an increase of Co^{2+} concentration and the value of enthalpy for conduction decreases with an increase of dopant concentration (Table I). Murphy also observed a similar behavior with Ba^{2+} dopant.

Mechanism for Conduction and Diffusion Processes

The discussion of the results of ADP and KDP crystals clearly indicates that the temperature region -70 to $+165^\circ\text{C}$ is due neither to extrinsic nor due to intrinsic regions. If this temperature region represented an intrinsic region, then the enthalpy of conduction should have been almost independent of the dopant concentration. On the other hand, if this were an extrinsic region, then an enthalpy of 0.71 eV is too high to be considered as the enthalpy for migration of protons, especially when the enthalpy for formation of an extrinsic defect is only 0.1 eV.

The second pertinent question to ask is, what is the meaning of (impurity-vacancy) complexes and the significance of H_s and H_m enthalpies in these crystals. Let us consider the cause for the formation of such complexes. Each divalent Co(II) impurity is expected to create at least one proton or cation vacancy. The vacancy in the neighborhood of Co(II) can form an impurity-vacancy complex. If such complexes are present in the ADP and KDP single crystals, then the isotherm treatment should not have given a negative value for K_a and H_a (Table I). Moreover, if H_s and H_m were representing the enthalpy for formation of defect and the enthalpy for migration of defect, H_s should not have been smaller than H_m (Table I). On the other hand these results could be valid, if the dopant, instead of creating only a vacancy, might also be doing something else in the crystal and H_s and H_m might be referring to some other phenomena rather than simply to the formation and migration of enthalpies. Under these circumstances, the L-, D-, or A-type defects may not be responsible for this conduction process in these crystals.

Blinic *et al.* (20, 21), on the other hand, have proposed from their NMR studies that in the KDP crystal the H_2PO_4^- ion can reorient around the threefold axes of the PO_4 tetrahedron, by which the proton can jump from one site to another. It can therefore be assumed that the H_2PO_4^- group can rotate along any of its four axes of rotation to give a threefold rotation in space. These rotations can also be

assumed to be either a bidirectional axial type or a clockwise rotation type. Nevertheless, out of all possible rotations, the H_2PO_4^- group can rotate along the axis which contains no covalent hydrogen atom because rotation along such an axis will bring two hydrogen atoms close to each other forming a situation of O-H-H-O (Fig. 9a). This situation (analogous to the D-defect) cannot exist because KDP and ADP have a double potential well with a distance between two possible sites of only 0.4 Å which is too small to accommodate two protons in the same O-H-O bond (14) and would require a high enthalpy. Therefore if such a rotation occurred, the H_2PO_4^- group would be forced to revert back to its initial position by the bidirectional axial-type process. Moreover, the situation developed by such a rotation would not help in allowing the protons to transfer from one H_2PO_4^- group to the other (Fig. 9a).

When the rotation occurs along axes containing covalent hydrogen atoms a situation of the type OHO arises (Fig. 9b). It should be mentioned that before the rotation of the H_2PO_4^- group, a hydrogen atom of $\text{P}^1\text{-O}^1\text{-H}^1$ was attached to a different PO_4 group and only after the rotation did it form the new bond of a P-O group. Similarly, in the case of $\text{P}^2\text{-O}^2\text{-H}^1$ (which was hydrogen bonded to a different PO_4^- group), only after rotation through the P-O axis did it join with the $\text{P}^1\text{-O}^1\text{-H}^1$ bond. Under these rotations, the proton has an opportunity to migrate to other H_2PO_4 groups. Since the rotation of the H_2PO_4^- group is of the bidirectional type, there is an equal probability for the proton (which has migrated to the next adjacent H_2PO_4^- group) to come back to its initial position. This to-and-fro motion of

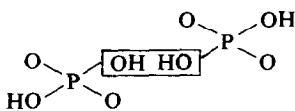


FIG. 9a.

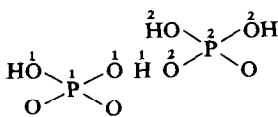


FIG. 9b.

the proton can be restricted to one direction by applying a dc potential across the crystal. The details of the sequential process under the electric field are shown in Fig. 10. As soon as the dc potential is applied, all the hydrogen atoms present near the surface of the crystal are discharged and throughout the crystal a transfer of protons occurs (in the direction of field) such that all hydrogen-bonded atoms become covalent-bonded hydrogen and vice versa (steps 1 and 2). Then the three-fold rotation along P-O axis containing a covalent hydrogen takes place. This brings the hydrogen atom from inside the crystal to the surface for hydrogen to discharge (steps 3 and 4) at the electrode. These processes occur in a synchronized manner throughout the crystal, such that the incoming proton always finds the next site empty. This mechanism gives a transfer of the proton in a helical-type movement in the crystal along the c axis (Fig. 11). Figures 10(5, 6) show the effect of rotation along the forbidden P-O axis (containing no covalent hydrogen) which would result in the formation of an unstable O-H-H-O situation.

In addition, since these rotation processes are of a cooperative type, the presence of the impurity in the crystal structure can affect the rotation of many H_2PO_4^- groups. The ESR studies of the Cu^{2+} -doped KDP crystal by Olani and Makishima (22) support this argument. They found that one atom of Cu^{2+} affects as many as eight positions of hydrogen atoms in the crystal. Therefore, the frequency of rotation of the H_2PO_4^- group can be expected to increase by the addition of the divalent dopant. If the conduction process is controlled by the frequency of rotation of H_2PO_4^- the conductivity should also increase with the increase of dopant concentration and the enthalpy of rotation (i.e., enthalpy of conduction) should decrease with the increase of conductance. This is what we have observed (Table I). This rotation mechanism requires no enthalpy for the formation of the defect ($H_s = 0.1$ eV) nor does it require any break in the conductivity plot. Both are in agreement with our experimental observations.

The diffusion process in the absence of an electrical field would be controlled by two factors, the first being the enthalpy for the

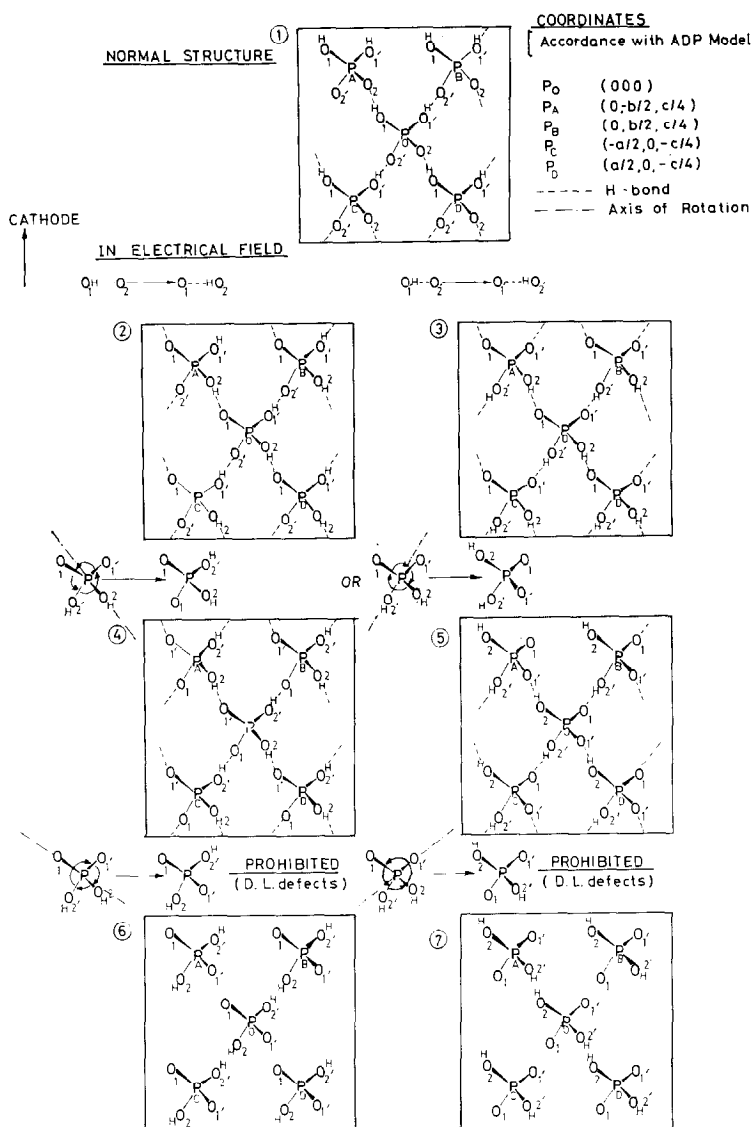
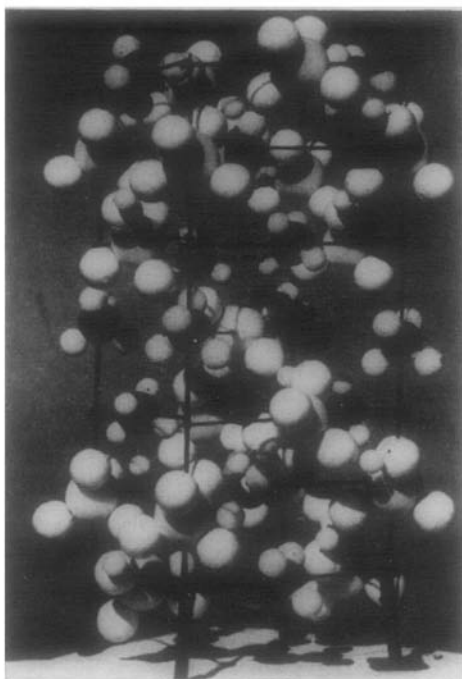


FIG. 10. Synchronized rotation mechanism for proton conduction in acid phosphates.

exchange of $\text{O}^1\text{-T}\cdots\text{O}^2$ to $\text{O}^2\text{-T}\cdots\text{O}^3$ and the second being the probability for the forward direction exchange. The latter is important when the bidirectional-type rotation of H_2PO_4^- is in operation. This can be explained as follows. After the rotation of the HTPO_4 group, the tritium atom has come near the other group. It will now try to attach with $\text{H}_2\text{P}^2\text{O}_4^-$ to form the HTP^2O_4^- group making the former group H_2^1PO_4 . Since HTP^2O_4^- is under a bidirectional axial-type rotation,

either it can transfer tritium to the next-nearest $\text{H}_2\text{P}^3\text{O}_4$ group or it can transfer back to the first $\text{H}_2\text{P}^1\text{O}_4^-$ group. The probability of the latter process is greater when the rotation of the HTP^2O_4 group is not properly synchronized with the rotation of the $\text{H}_2\text{P}^3\text{O}_4$ group or there is not enough tritium concentration to force the transfer of the tritium toward its lower concentration region. In either case, the exchange of tritium will depend upon the enthalpy of exchange of tritium from the



MODEL OF ADP.

Big white ball - P
 Medium white ball - O
 Small white ball - H
 Black ball - N
 Coordinates of central PO_4 group (000)

Direction of Axes-

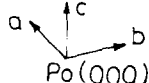


FIG. 11. Model of ADP.

$P^1-O-T \cdots O-P^2$ to the $P^2-O-T \cdots O-P^3$ bond. This type of exchange is expected to have a very low energy of activation. This is what we have observed here.

Conclusion

The conduction process in ADP and KDP crystals is controlled by the enthalpy for rotation of the phosphate group and not by L-, D-, or A-type defects because the latter defects require the presence of an extrinsic as well as an intrinsic region in the conductivity plot. The addition of dopant makes the $H_2PO_4^-$ group free of a hydrogen atom, and thus increases the frequency of the rotation of the

phosphate group. Because of this factor, the conductance value increases and the enthalpy of conduction decreases with an increase of the dopant concentration. It is also suggested that diffusion studies give the measurement of enthalpy of the proton exchange from one phosphate group to another, whereas conduction studies give the enthalpy for the rotation of the phosphate group only. The high enthalpy of rotation is canceled in the diffusion studies because the enthalpy for clockwise rotation would be the same magnitude as but of opposite sign to the enthalpy for the anticlockwise rotation (bidirectional-type rotation), leaving behind only the enthalpy of proton migration (i.e., from one to another phosphate group). This model, however, will be tried with other crystals to prove its validity.

Acknowledgments

One of us (A.K.K.) wishes to thank the UGC (India) for providing a research assistantship and a special grant, without which this work could not have been completed. Thanks are also due to Professor H. J. Arnikar for his constant encouragement in this work.

References

1. R. S. BRADLEY, D. E. MURO, AND S. L. ALI, *J. Inorg. Nucl. Chem.* **32**, 2513 (1970).
2. V. H. SCHMIDT AND E. A. VEHLING, *Phys. Rev.* **126**, 447 (1962).
3. L. B. HARRIS AND G. J. VELLA, *J. Appl. Phys.* **37**, 4294 (1968).
4. M. O'KEEFFE AND C. T. PERRINO, *J. Phys. Chem. Solids* **28**, 211 (1967).
5. M. O'KEEFFE AND C. T. PERRINO, *J. Phys. Chem. Solids* **28**, 1068 (1967).
6. W. P. MASON, "Piezoelectric Crystals and their Application to Ultrasonics" p. 140, Van Nostrand, New York (1950).
7. E. J. MURPHY, *J. Appl. Phys.* **35**, 2609 (1964).
8. J. M. POLLOCK AND M. SHARAN, *J. Chem. Phys.* **51**, 3604 (1969).
9. L. B. HARRIS AND G. J. VELLA, *J. Chem. Phys.* **58**, 4550 (1975).
10. C. T. PERRINO AND P. WENTRCEK, *J. Solid State Chem.* **10**, 36 (1974).
11. E. P. KHAIRETDINOV, V. V. BOLDYREV, AND A. I. BURSHEIN, *J. Solid State Chem.* **10**, 288 (1974).
12. L. GLASSER, *Chem. Rev.* **75**, 21 (1975).

13. T. M. HERRINGTON AND L. A. K. STAVELEY, *J. Phys. Solids* **25**, 921 (1974).
14. G. E. BACON AND R. S. PEASE, *Prof. Roy. Soc. A.* **230**, 359 (1955).
15. P. HOFFMANN AND K. H. LIESER, *Sanderuckans Radiochemica Acta* **16**, 96 (1971).
16. J. WEIS, *Krist. Tech.* **6**, 69 (1971).
17. A. B. LIDIARD, "Handhuch Der Physik" (Springer-Verlag, Berlin), **20**, 246 (1957).
18. YU. M. POPLANKO, I. S. REZ., N. V. GORBOKON'S, AND E. N. DIMAROVA, *Soviet Phys-Crystallogr.* **17**, 595 (1972), *Kristallografiya* **17**, 620 (1972), *Chem. Abstr.* **77**, 671735 (1972).
19. S. J. KIEHL AND G. H. WALLACE, *J. Amer. Chem. Soc.* **49**, 375 (1927).
20. R. BLINC, J. STEPISMILK, M. JAMSEK-VILFAN, AND S. ZUMAR, *J. Chem. Phys.* **54**(1), 187 (1971).
21. R. BLINC AND J. PIRS, *J. Chem. Phys.* **54**(4), 1535 (1971).
22. A. OLANI AND S. MAKISHIMA, *J. Phys. Soc. Japana* **26**, 85 (1969).